The American Journal of Pathology, Vol. 171, No. 4, October 2007

DOI: 10.2353/ajpath.2007.070388

Immunopathology and Infectious Disease

Autoimmune Dacryoadenitis of NOD/LtJ Mice and Its Subsequent Effects on Tear Protein Composition

Máire E. Doyle,*† Lori Boggs,* Robert Attia,* Lauren R. Cooper,* Daniel R. Saban,* Cuong Q. Nguyen,* and Ammon B. Peck*†‡

From the Department of Oral Biology, and the Center for Orphan Autoimmune Diseases,‡ College of Dentistry, and the Department of Pathology, Immunology, and Laboratory Medicine,† College of Medicine, University of Florida, Gainesville, Florida*

Sjögren's syndrome (SjS) is a human autoimmune disease characterized by exocrine dysfunction resulting from chronic autoimmune attack primarily against the lacrimal and/or salivary glands. Although, we previously established a good correlation between SjS in humans and autoimmune exocrinopathy in NOD/LtJ mice an in-depth evaluation of lacrimal gland disease in the NOD/LtJ mouse has remained limited. This leaves a major gap in our understanding of the dacryoadenitis/keratoconjunctivitis sicca in this model. Here we characterize the development of the autoimmune dacryoadenitis in NOD/LtJ and NOD.B10-*H2*^{b} mice in comparison with age- and sex-matched nonautoimmune CD1 mice. We observed a decline in tear production beginning at 8 weeks of age in both NOD/LtJ and NOD.B10-*H2*^{b} mice, continuing throughout the 40 to 46 weeks studied. This correlated with a quantifiable increase in mixed T- and B-lymphocyte infiltrations in the extraorbital lacrimal glands. In addition, temporal differences in tear protein expression between NOD/LtJ and CD1 mice were identified using two-dimensional gel electrophoresis and tandem mass spectrometry. Thus, using this model we can identify potentially important pathophysiological mechanisms of the autoimmune attack and possible diagnostic markers for development of SjS-associated dacryoadenitis. ***(Am J Pathol 2007, 171:1224–1236; DOI: 10.2353/ajpath.2007.070388)***

Dry eye diseases, or syndromes, result from changes in the tear flow rate, the composition of the tears, or both.[1] Underlying causes of these alterations include the natural aging process, autoimmune attack against one or more of the multiple secretory tissues/glands of the eye, irradiation, injury, and/or surgical procedures.[2] In general, these causes seem to result from a loss of exocrine cell mass, an onset of exocrine cell senescence or refractivity, and/or loss of, neural regulation of the ocular secretory reflex arc.[3] One of the more severe forms of dry eye disease is associated with Sjögren's syndrome (SjS).[4] SjS is a human disease characterized by exocrine gland dysfunction resulting from the action of an autoimmune response.[4] Primary SjS is characterized by a chronic autoimmune attack against the lacrimal and salivary glands, whereas secondary SjS is marked by an autoimmune attack against the lacrimal and/or salivary glands in the presence of another autoimmune disease, often a connective tissue disease.[5] In addition to the primary sites of SjS, (ie, the lacrimal and salivary glands), other tissues that can be affected include the entire gastrointestinal tract, the skin, the lungs, the liver, and the vagina.[6] Fibromyalgia-like symptoms are also often associated with SjS. As with several other autoimmune connective tissue diseases, there exists a sexual dimorphism in SjS with women affected 15 to 20 times more frequently than men,[7] suggesting a role for sex hormones in disease susceptibility,[8–10] possibly related to the relative balance between androgen and estrogen.[11]

Throughout the past 2 decades, a variety of mouse models exhibiting various aspects of SjS have been advanced

Supported in part by the National Institutes of Health (Public Health Service grants DE013769, DE014344, and DE015152 to A.B.P. and postdoctoral fellowship grant T32 DE07200 to C.Q.N.) and the University of Florida Center for Orphan Autoimmune Diseases (to M.E.D.).

Accepted for publication June 26, 2007.

A.B.P. has financial interest in Ixion Biotechnology, Inc. There has been no financial or other material support for this study from Ixion or any other commercial source.

Supplemental material for this article can be found on *http://ajp.amjpathol.org.*

Current address of D.R.S.: The Schepens Eye Research Institute, Harvard Medical School, Boston, MA.

Address reprint requests to Dr. Máire E. Doyle, Division of Endocrinology, Johns Hopkins Bayview Medical Center, 5200 Eastern Ave., Mason F. Lord Center Tower, Suite 432, Baltimore, MD 21224. E-mail: mdoyle1@jhmi.edu.

and investigated in an attempt to identify the nature of this autoimmune disease.[12] Typically, these mouse models show lymphocyte infiltration of the exocrine glands, increased expressions of proinflammatory cytokines, generation of unique autoantibodies [especially ANAs, anti-α-fodrin, and anti-muscarinic acetylcholine type-3 receptor (M_3R) antibodies], and eventually decreased saliva flow rates.[13–24] Strains that have been extensively studied include NZB/NZW F1-hybrids,[25] MRL/*lpr*,[26] NOD/LtJ,[19] NFS/*sld*,[27] IQI/Jic,[28,29] the C57BL/6.NOD-*Aec1Aec2* congenic line,[12] the *Id3* gene knockout,[30] the *aromatase* gene knockout,[31] and *Baff* gene knockin mice.[32] Although each strain has been reported to resemble features of SjS in human patients, none recapitulate completely the pathological characteristics of the human disease. Nevertheless, one of the more interesting and well-studied models of SjS is the nonobese (NOD) mouse, which not only closely mimics the human disease but has a large number of congenic partner gene knockout strains, eg, NOD-*scid*, NOD.*Ifn*$\gamma^{-/-}$, NOD.*IL2*$^{-/-}$, NOD.*IL4*$^{-/-}$, NOD.*IL10*$^{-/-}$, NOD.*Ig*$\mu^{-/-}$, and NOD.*Stat6*$^{-/-}$, permitting investigations into the role of individual genes in the development and onset of SjS-like disease in this model.[14–17] Studies using these NOD-derived mice have led to the hypothesis that SjS-like disease is divided into three distinct consecutive phases.[17–20] In phase 1 (initiation of glandular pathology), a number of aberrant genetic, physiological, and biochemical activities associated with retarded salivary gland organogenesis and increased acinar cell apoptosis occur sequentially before and independent of detectable autoimmunity.[20] In phase 2 (onset of autoimmunity believed to result from acinar cell apoptosis), leukocytes expressing proinflammatory cytokines infiltrate the exocrine glands, establishing lymphocytic foci, first of T-cell clusters followed by recruitment of B lymphocytes.[21,22] In phase 3 (onset of disease), loss of salivary and lacrimal gland secretory functions occur, most likely the result of (auto-)antibodies reactive with the M_3Rs.[13,14,23,24] Overall, then, there is little doubt that onset of SjS-like disease in the NOD mouse model represents a progressive and chronic autoimmune process that slowly leads to exocrine gland dysfunction.

Although the pathology of autoimmune xerostomia has been extensively investigated in numerous mouse models of SjS, especially NOD/LtJ- and NOD-derived mouse strains, far less information has been published on the autoimmune xerophthalmia in these mice. Thus, in the present study, we present results of a comprehensive study designed to identify temporal changes in the dacryoadenitis lesions within the lacrimal glands and protein physiology of tears exhibited by NOD/LtJ and NOD.B10-*H2*^{b} mice during and after disease onset. NOD.B10-*H2*^{b} mice, in which the diabetes susceptibility gene locus, *Idd1*^{S}, has been replaced with a diabetes resistance gene locus, *Idd1*^{R}, have been included in the present study to eliminate any effects diabetes might have on the SjS-like disease exhibited by NOD/LtJ mice.[33] Results are presented that reveal the extent of the autoimmune attack against the various ocular-associated exocrine glands and the subsequent consequences of this autoimmune attack in altering the composition of tear proteins.

Materials and Methods

Animals

Breeding pairs of NOD/LtJ and NOD.B10-*H2*^{b} mice were originally purchased from Jackson Laboratories (Bar Harbor, ME), and breeding pairs of CD-1 mice were purchased from Charles River Laboratory (Wilmington, MA). All mice were bred and maintained within the Department of Pathology's Mouse Facility at the University of Florida, Gainesville, FL. Because dacryoadenitis is reported to be more severe in males than females of NOD-derived strains, all studies reported here were conducted on male mice. Euthanasia was performed by cervical dislocation after anesthetization with isoflurane. The studies reported herein were performed according to the Association for Research in Vision and Ophthalmology Statements for the Use of Animals in Ophthalmic and Vision Research, approved by the University of Florida's Institutional Animal Care and Use Committee and overseen by Animal Care Services' veterinarians.

Measurement of Tear Volumes

To reduce movement and stress during measurement of tear flow rates, the mice were lightly anesthetized using isoflurane. The mice were injected with pilocarpine hydrochloride (4.5 mg/kg in saline) and allowed to rest comfortably for 10 minutes. After the resting period, tear volumes were measured by carefully placing the bent end of a Zone-Quick phenol red thread (FCI Ophthalmics, Pembrooke, MA) at the intercanthus of one eye and held in place with sterile forceps for 20 seconds, a modification of the procedure described by Hamano and colleagues.[34] On removal of the thread, the length of the red area was measured using the scale provided and recorded. The red portion of the thread containing the tear sample was then cut into small fragments (~2 to 3 mm in length), placed in an equivalent volume of phosphate-buffered saline (PBS), and stored at −80°C.

Histological Evaluation

Submandibular and lacrimal glands were removed from euthanized mice, placed in 10% phosphate-buffered formalin for 24 hours, and then processed and embedded in paraffin. The embedded tissues were sectioned at 5-μm thickness and mounted onto microscope slides. Slides were deparaffinized and rehydrated in a graded series of ethanol. Tissue sections were stained with Mayer's hematoxylin and eosin (H&E) dye and observed at the magnifications listed in the figure legends. The extent of lymphocytic infiltration in the extraorbital lacrimal glands was assessed by two methods. First, the numbers of lymphocyte foci containing more than 50 cells were determined for each section. Second, the severity of the inflammatory lesions were classified into five grades (0 to 4) using the criteria defined by Takada and colleagues.[28,29] In brief, this classification is as follows: 0, no

visible change; 1, mild accumulation of mononuclear cells within the interstitium; 2, focal accumulation of mononuclear cells without any parenchymal destruction; 3, focal accumulation of mononuclear cells with parenchymal destruction; and 4, extensive infiltration of mononuclear cells with severe tissue damage. Each extraorbital lacrimal gland was graded as a whole and the results presented as the mean of the number of foci per full glandular section. The glands themselves are extremely small, allowing only for a very few sections to be cut. We examined several sections in one gland and found that the initial two to three sections cut were representative of those generated from the entire gland.

Immunofluorescent Staining for T and B Cells

Tissue sections prepared as described above were washed 5 minutes with PBS at 25°C, then incubated 1 hour with blocking solution containing normal rabbit serum diluted 1:50 in PBS. Rat anti-mouse B220 (BD Biosciences PharMingen, San Diego, CA) diluted 1:10 and goat anti-mouse CD3 (Santa Cruz Biotechnology, Santa Cruz, CA) diluted 1:50 were added to individual sections for 1 hour at 25°C. The slides were washed three times with PBS for 5 minutes per wash followed by a 1-hour incubation at 25°C in a mixture of secondary antibodies [Texas Red-conjugated rabbit anti-rat IgG (Biomeda, Foster City, CA) diluted 1:25 and fluorescein isothiocyanate-conjugated rabbit anti-goat IgG (Sigma Chemicals, St. Louis, MO) diluted 1:100]. The slides were thoroughly washed with PBS, treated with Vectashield DAPI-mounting medium (Vector Laboratories, Burlingame, CA), and overlayed with glass coverslips.

Tear Protein Preparation for Two-Dimensional Differential Gel Electrophoresis (2D DIGE)

Tear proteins were precipitated with 9 vol of ice-cold 10% TCA, 80% acetone, and 20 mmol/L dithiothreitol overnight at −20°C. Protein precipitate was then washed with 80% ice-cold ethanol and air-dried for 5 minutes before being dissolved in sample buffer containing 10 mmol/L Tris buffer, pH 8.5, 8 mol/L urea, 2 mol/L thiourea, 4% (w/v) CHAPS, and 0.2% sodium dodecyl sulfate. The urea/thiourea protein solution was then clarified at 40,000 × *g* for 30 minutes before dialysis in same urea/thiourea buffer overnight at 4°C to remove salt and small molecules. Protein concentration was determined using a 2D Quant kit (Amersham Biosciences, Arlington Heights, IL) after tear protein has been precipitated to remove urea and detergent. Samples were then used either for an analytical comparison of differentially expressed proteins or for preparative experiments for protein characterization as outlined below.

Minimal CyDye Labeling for 2D DIGE

Control mouse tear proteins (50 μg) were labeled with Cy3, whereas equal amounts of experimental tear proteins were labeled with Cy5. Excess CyDye was quenched with 10 mmol/L lysine before the labeled proteins were reduced with dithiothreitol and carrier ampholyte pH 3 to 10 (1% v/v) added. For matrix-assisted laser desorption/ionization time-of-flight, unlabeled pooled tear proteins were mixed with the labeled proteins and processed as described below. Immobilized pH 3 to 10 gradient (IPG) strips (Amersham Biosciences, Inc.) were rehydrated with the Cy-Dye-labeled samples, according to the manufacturer's guidelines (Amersham Biosciences, Inc.). First-dimension isolectric focusing was performed using an IPGphor apparatus (Amersham Biosciences, Inc.). After isolectric focusing, the protein in the IPG strips was reduced with 100 mmol/L dithiothreitol and then alkylated with 2.5% iodoacetamide. The IPG strips were mounted with 0.5% agarose solution onto an 8 to 16% Tris glycine-sodium dodecyl sulfate polyacrylamide gel, and protein spots were separated with running buffer. Fluorescence images of both control and experimental protein maps were acquired with green (532 nm) and red (633 nm) lasers. The difference in protein expression between control and experimental samples were analyzed with Nonlinear Dynamc's Phoretix 2D Evolution software (Durham, NC). Features resulting from nonprotein sources (eg, dust particles and scratches) were filtered out. The analyses calculated abundance differences between samples run on the same gel, and proteins demonstrating a twofold or more difference or proteins unique to one sample were chosen for protein identification.

Table 1. Temporal Changes in Tear Volumes of NOD/LtJ, NOD.B10-*H2*^{b}, and CD-1 Mice Compensated for Body Weight

Mouse strain	Age at first collection (weeks)	*n*	Tear volume collected (mm)	Age at second collection (weeks)	*n**	Tear volume collected (mm)	Percent decrease in original tear volume†
NOD/LtJ	4.0	8§	1.60 ± 0.10	40	4	0.70 ± 0.18	56%; $P < 0.01$‡
NOD.B10-*H2*^{b}	5.0	6	1.54 ± 0.38	52	4	0.73 ± 0.13	53%; $P < 0.05$
CD-1	4.5	8	1.17 ± 0.09	35	7	1.12 ± 0.07	4.3%; P = n.s.

*Diabetic NOD/LtJ mice were not included in the second collection.
†The reduction in tear volume between final and initial time points as a percentage of the initial volume.
‡*P* values determined by Student's *t*-test.
§Animals not shown in final values had expired during the course of the experimental observation.

Spot Excision

After imaging, each gel was counterstained with Coomassie Blue. Visible spots, and a control gel piece of comparative size, were excised and stored in 25% methanol for protein identification. Sodium dodecyl sulfate was removed from the gel fragments by washing in acetonitrile, and then samples were dehydrated with pure acetonitrile. The supernatant was removed and rehydrated in a minimal volume of ammonium bicarbonate, a process repeated until the gel was colorless. The remaining gel piece was dried in a Speedvac and reduced by rehydrating in dithiothreitol (45 mmol/L). Any supernatant liquid was removed, and freshly prepared iodoacetamide was added immediately to alkylate the proteins in the gel piece. After several washes in a 1:1 mixture of acetonitrile/ammonium bicarbonate, each sample was dried and subjected to trypsin digestion. The enzyme solution was removed and replaced with the enzyme diluent overnight. The supernatant was then removed and stored in a clean tube and the reaction stopped by adding formic acid to a final concentration of 5%.

Liquid Chromatography Tandem Mass Spectrometry (LC/MS/MS-Protein Characterization)

A capillary trap in combination with a MicroPro gradient solvent delivery system (Eldex, Napa, CA) was used to concentrate and desalt the sample before LC/MS/MS analysis. Gradient flow rates between 200 to 300 nl/minute were attained by splitting a flow of 5 μl/minute supplied by the high performance liquid chromatography pump. After column equilibration in 3% solvent A (0.1% acetic acid in 95% water/5% acetonitrile), the sample was injected. After isocratic solvent delivery for 5 minutes, a linear gradient was performed for 60 minutes to 30% solvent B (0.1% acetic acid in 95% acetonitrile/5% water). Nanoflow electrospray ionization experiments were performed by interfacing a PicoView (New Objective, Woburn, MA) ion source to a quadrupole ion trap instrument operated with the Xcalibur (version 1.3) data system software. Electrospray ionization spray voltage and capillary temperature were maintained at 1.2 kV and 180°C, respectively. Full-scan and product-ion mass spectra were obtained using the data-dependent acquisition feature in the Xcalibur software. Full-scan mass spectra were acquired from *m/z* 400 to 1800 using the automatic gain control mode of ion trapping (target ion count of 5×10^7). Tryptic peptide ions that exceeded the threshold level of 1×10^5 counts were subjected to collision-induced dissociation at 2.0-u isolation width and 1.75 V-activation amplitude with helium as target gas.

Mass Spectral Data Analyses

The algorithm SEQUEST was used to facilitate analysis of the Xcalibur data. Peptide spectra were compared against entries in the IPI mouse v1.31 (Oct 2004) database. Results from SEQUEST were considered significant when the delta correlation value (ΔCn) was equal to or greater than 0.08 and when the cross-correlation (Xcorr) between the observed mass spectrum and the theoretical candidate mass spectrum was equal to or greater than 1.8 for a peptide ion with a single positive charge, 2.0 for a double positive charge, and 3.0 for an ion with three positive charges.

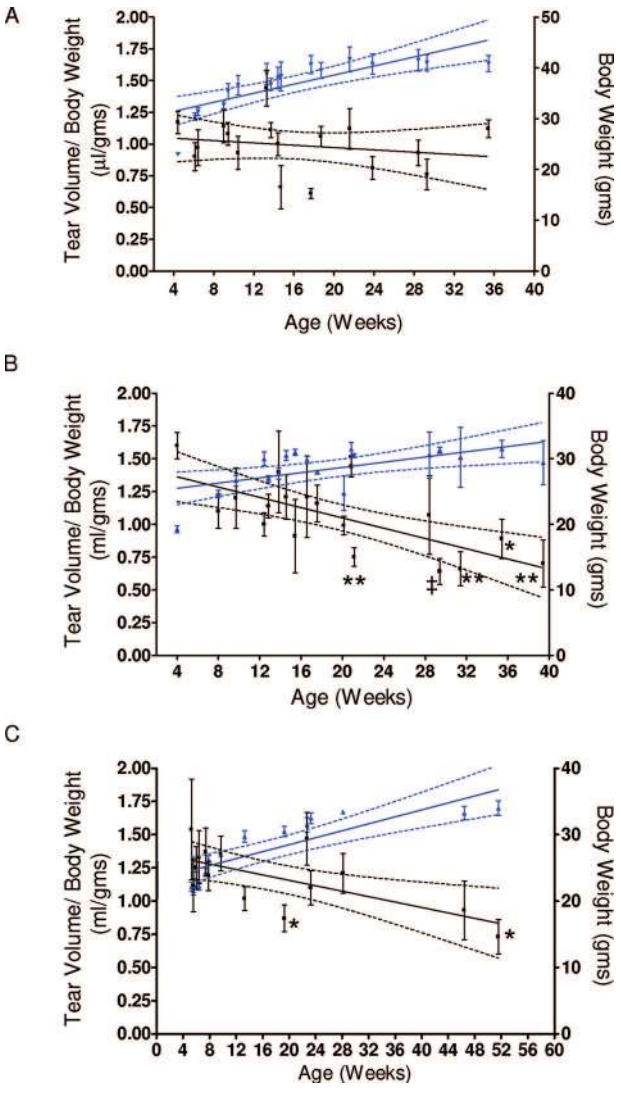

Figure 1. Temporal changes in pilocarpine-stimulated tear volumes. Tears were collected from the eyes of CD-1 (**A**), NOD/LtJ (both diabetic and nondiabetic) (**B**), and NOD.B10-*H2*^{b} (**C**) male mice at the ages indicated using Zone-Quick Phenol Red Threads placed in the intercanthus of one eye. The tear flow rates (black lines and left *y* axis values) were compensated for body weights measured at each collection time point. Body weights of the animals at each time point are shown (blue lines and right *y* axis). The dotted lines represent the 95% confidence band of the regression line generated from the tear flow rate and body weight data shown. Results are the means ± SEM (n = 3 to 8 mice per collection). *$P < 0.05$, **$P < 0.01$, and ‡$P < 0.001$ compared with tear volumes collected at 4 weeks of age. Statistically significant differences were calculated using one-way analysis of variance and Tukey's multiple comparison post hoc test.

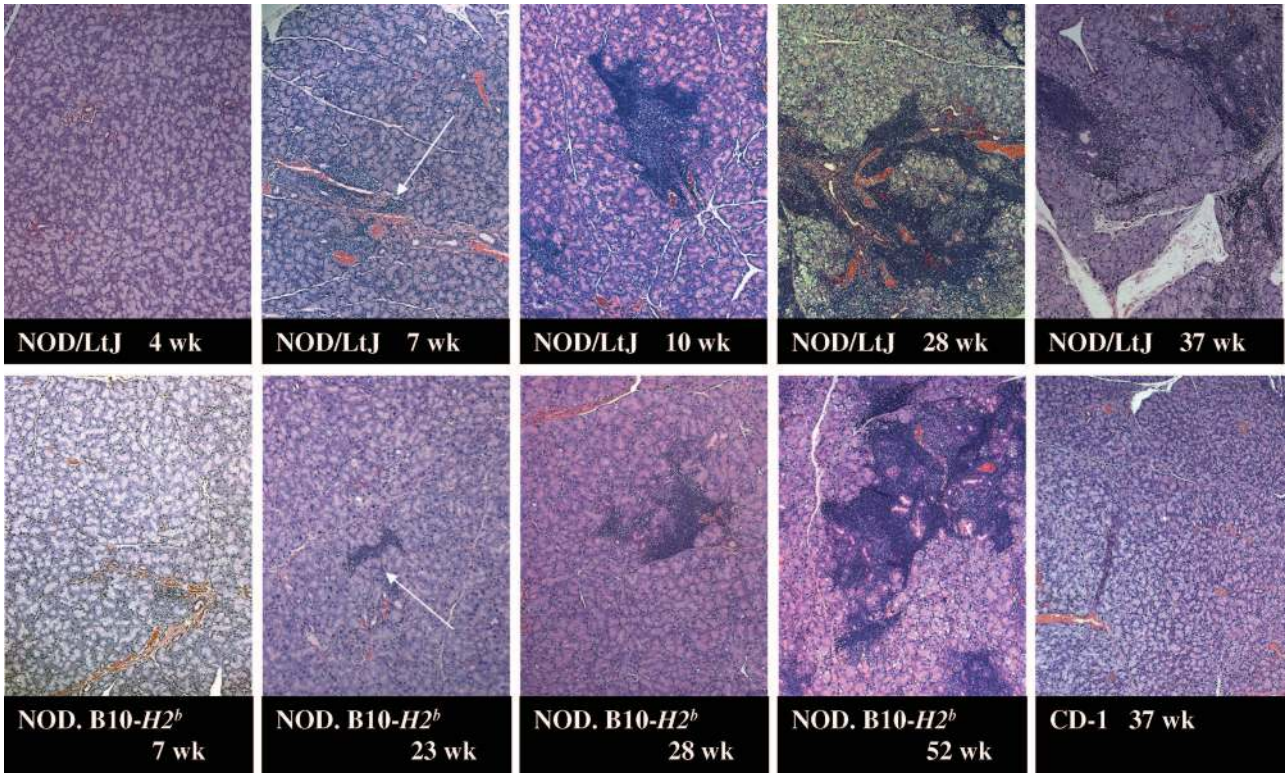

Figure 2. Cellular infiltration of leukocytic foci within the extra-orbital lacrimal glands of NOD/LtJ and NOD.B10-*H2*^{b} male mice. Extra-orbital lacrimal glands removed from groups of NOD/LtJ and NOD.B10-*H2*^{b} mice ranging in age from 7 to 52 weeks were fixed in 10% formalin. Each gland was serially sectioned (5-μm thickness) and histology performed on sections cut 50 μm apart. Each section was stained with Mayer's H&E dye. Representative photomicrographs showing the temporal increase in leukocyte infiltration of the lacrimal glands is presented. Lacrimal glands from CD-1 mice showed no infiltrates up to 37 weeks of age. Sections were scored according to the grading system presented in Materials and Methods and presented in Table 2. Original magnifications, ×200.

Statistical Analyses

Data are presented as the mean ± SE of the means. Differences between mean values for variables within individual experiments were compared statistically using the Student's *t*-test with Welch's correction or by analysis of variance and Tukey's multiple comparison post hoc test (as indicated in the text). *P* values were calculated by GraphPad Prism (GraphPad Software, Inc., San Diego, CA), and *P* values <0.05 were considered statistically significant.

Results

Development of Keratoconjunctivitis Sicca with Temporal Loss of Tear Flow Rates

Previously, we and others have shown that NOD/LtJ and NOD.B10-*H2*^{b} mice exhibit a 30 to 40% loss of lacrimal gland secretions between 8 and 24 weeks of age that correlates with the development of dacryoad-

Table 2. Histopathological Analysis of Lymphocytic Infiltration in the Extra-Orbital Lacrimal Glands of Male NOD/LtJ and NOD.B10-*H2*^{b} Mice

Mouse strain	Age (weeks)	*n*	Number of foci (per section of extra-orbital gland)*	Inflammatory lesion (grade)†
NOD/LtJ	4	9	0‡	0‡
	6 and 7	10	6.2 ± 1.4 (range, 0 to 12)	1.6 ± 0.2
	10	8	18.6 ± 2.1 (range, 12 to 28)	2.1 ± 0.1
	12 and 14	7	15.1 ± 2.8 (range, 7 to 26)	3.3 ± 0.2
	28	8	27.0 ± 3.3 (range, 18 to 40)	4.0 ± 0.0
	33	3	18.0 ± 2.6 (range, 14 to 23)	4.0 ± 0.0
	37	5	9.2 ± 2.9 (range, 5 to 13)	3.8 ± 0.3
NOD.B10	7 and 8	13	5.0 ± 1.1 (range, 0 to 11)	1.5 ± 0.2
	23	14	11.0 ± 1.6 (range, 4 to 26)	2.7 ± 0.1
	28	6	21.7 ± 3.8 (range, 11 to 36)	3.0 ± 0.0
	52	8	29.5 ± 3.2 (range, 19 to 48)	2.9 ± 0.3

*Foci were considered as independent, noncontiguous areas of lymphocytic infiltration with >50 cells.
†Grading of inflammatory lesions was assessed by scoring the condition of each tissue section as a whole, then averaging those values over the total number of tissue sections for the strain at each age.
‡Number of foci and grade of inflammatory lesion are expressed as mean ± SEM.

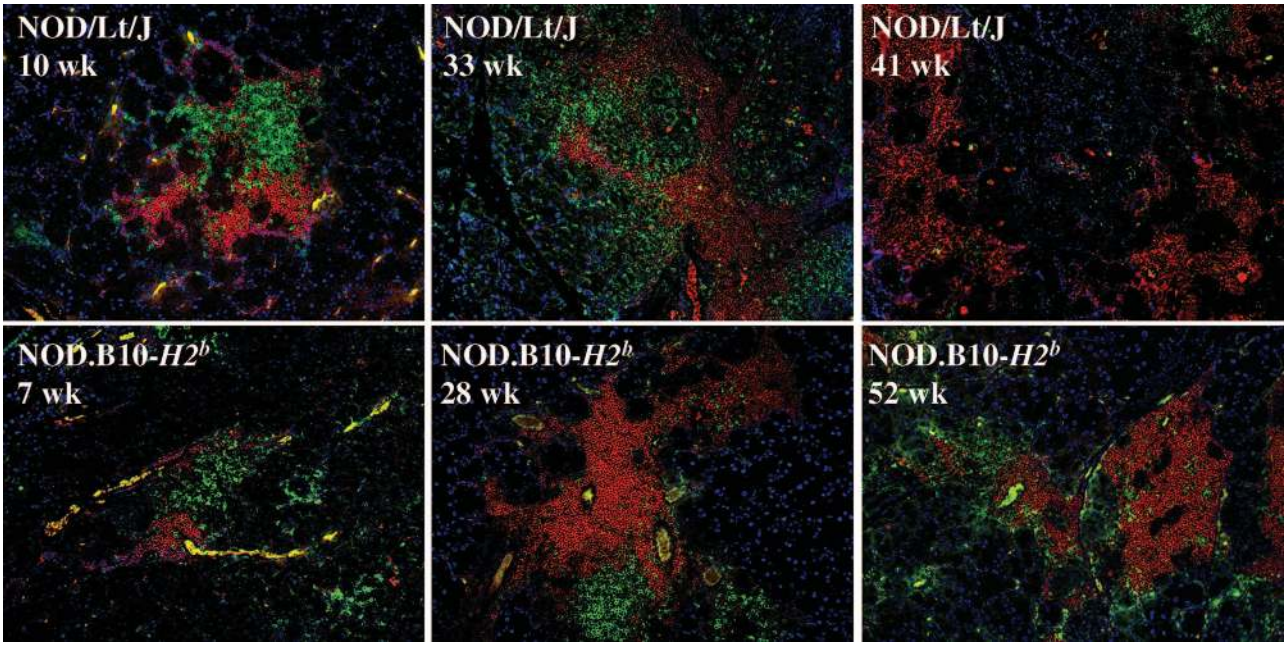

Figure 3. Differential staining for T and B lymphocytes within the leukocytic foci of lacrimal glands from NOD/LtJ and NOD.B10-*H2*^{b} male mice. Lacrimal glands removed from groups of mice at the ages shown were fixed in 10% formalin. Each gland was serially sectioned (5-μm thickness) and histology performed on sections cut 50 μm apart. Each section was stained with immunofluorescent antibodies for determining the distribution of B (anti-B220, red) and T cells (anti-CD3, green) in lymphocytic foci. The sections were counterstained with DAPI (blue). Original magnifications, ×200.

enitis.[11] To better characterize this particular feature of SjS-like disease in NOD/LtJ and NOD.B10-*H2*^{b} mice, tear secretions after stimulation with pilocarpine were determined at various intervals starting from 4 to 5 weeks of age and continuing for almost 1 year. As presented in Figure 1, B and C, stimulated tear vol-

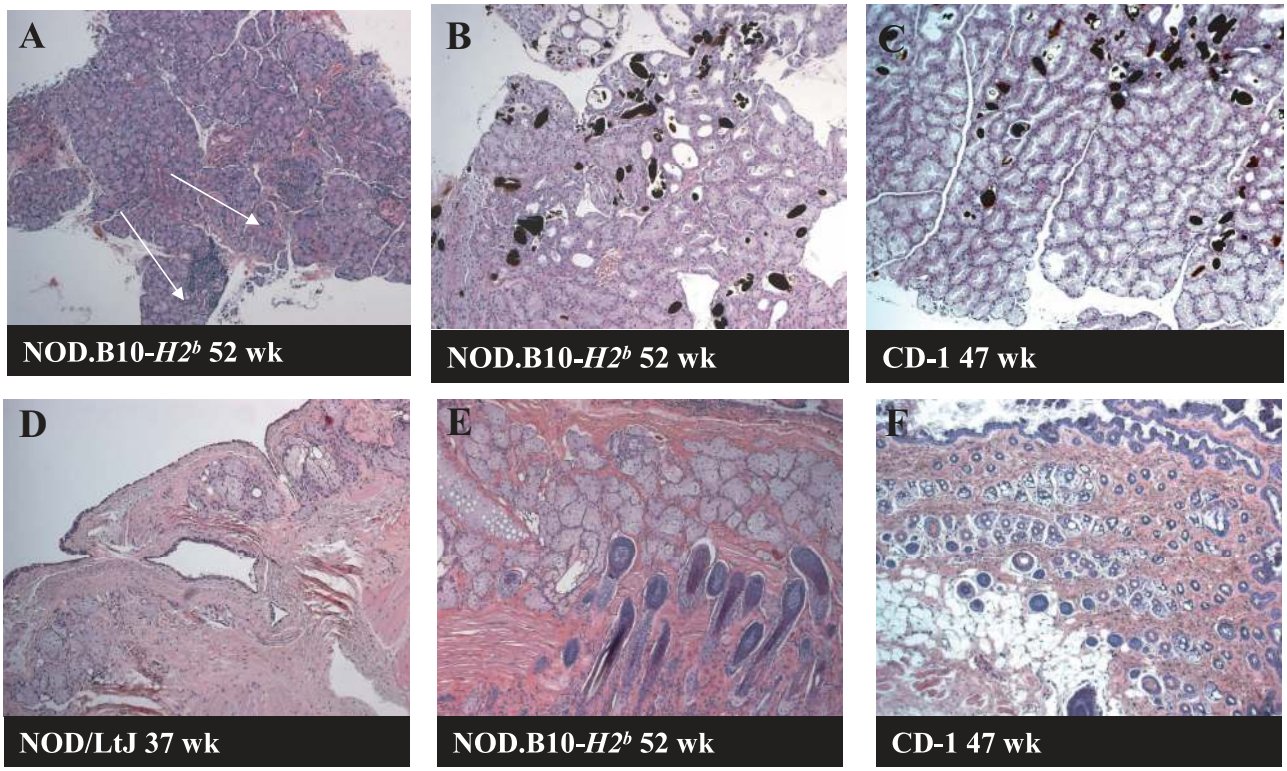

Figure 4. Lack of leukocytic infiltrates within the ocular-associated exocrine glands of NOD/LtJ and NOD.B10-*H2*^{b} male mice. The intraorbital lacrimal, meibomian, and Hardarian glands were removed from groups of NOD/LtJ, NOD.B10-*H2*^{b}, and CD-1 mice ranging in age up to 1 year, fixed in 10% formalin, serially sectioned (5-μm thickness), and histology performed on sections stained with Mayer's H&E dye. Although the intraorbital lacrimal glands of NOD/LtJ mice showed an occasional, small leukocyte infiltration at 1 year of age (**A**), neither the meibomian (**D**, **E**, and **F**) nor the Hardarian (**B** and **C**) glands showed signs of leukocytic infiltrations in any of the three strains tested. Original magnifications, ×200.

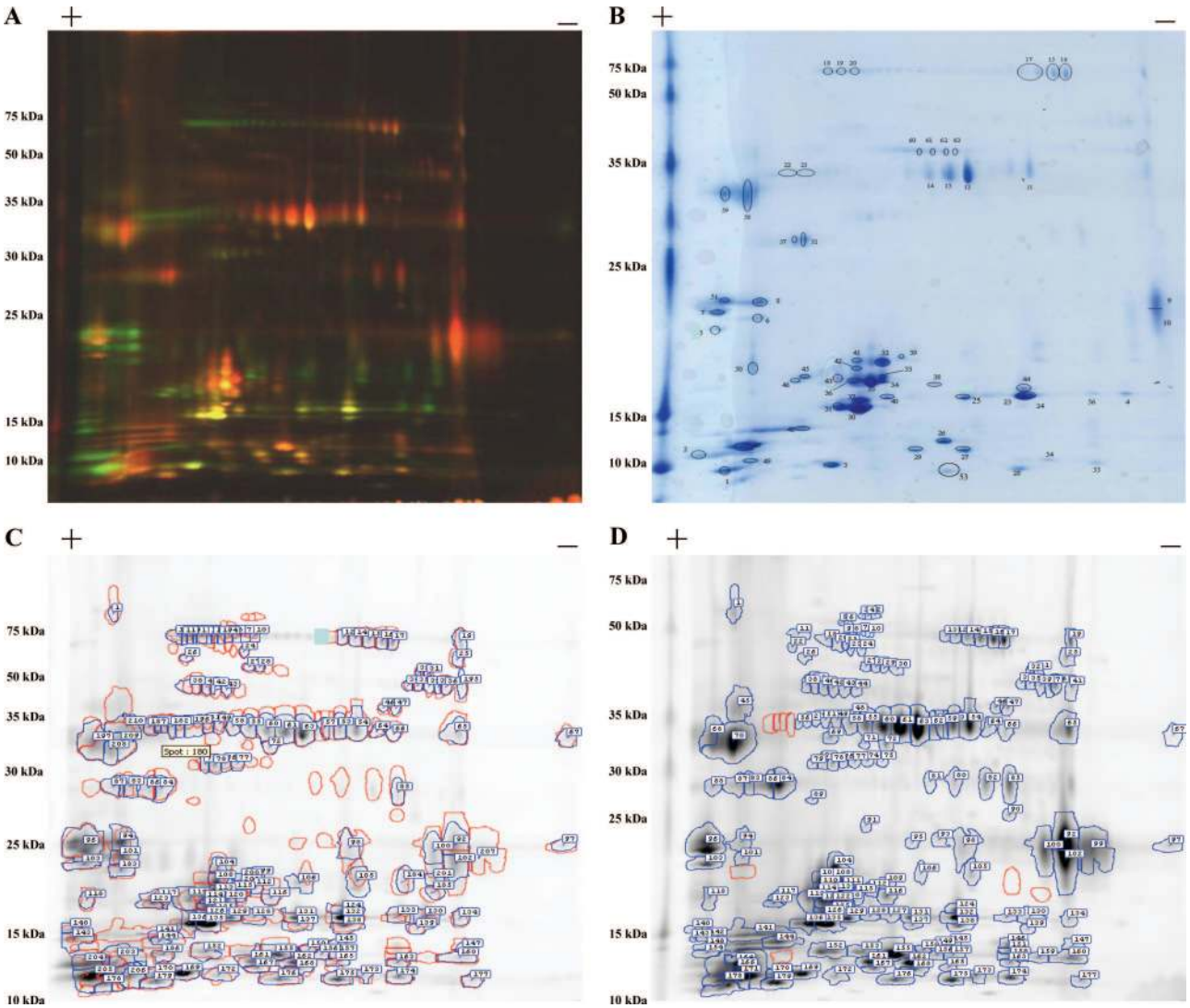

Figure 5. Changes in the proteome of lacrimal secretions from NOD/LtJ versus CD1 mice using 2D DIGE. Aliquots containing 50 μg of tear protein isolated from pilocarpine-stimulated tear fluids collected from NOD/LtJ and CD1 and mice 21 weeks of age were labeled with Cy5 and Cy3, respectively, subjected to isoelectric focusing followed by mass separation via sodium dodecyl sulfate-polyacrylamide gel electrophoresis. **A:** Computer generated image showing the fluorescently labeled samples run in the 2D DIGE gel showing the Cy5-labeled NOD/LtJ tear proteins in red and the Cy3-labeled CD1 tear proteins in green and those common to both in yellow. **B:** The gel in **A** was counterstained with Coomassie Blue, and dye spots were isolated and processed for tandem mass spectrometry. Peptide-ion mass spectra were generated using electron spray ionization and the operating software Xcalibur and matched to IPI mouse database entries using the SEQUEST search algorithm. Changes in protein levels were quantified and compared using Nonlinear Dynamc's Phoretix 2D Evolution software. Numbers represent the spots chosen for identification. The major proteins (ie, those identified by two or more peptide-ion mass spectra) identified from the 63 spots chosen are shown in Table 4. **C:** Computer-generated scan of the gel in **A** highlighting in red the proteins unique to the CD1 tear sample. **D:** Computer-generated scan of the gel in **A** highlighting in red the spots unique to the NOD/LtJ tear sample.

umes (standardized to the animals' weights) between the initial and final tear volume produced by the NOD/LtJ and NOD.B10-*H2*^{b} mice decreased to 56 and 53%, respectively (Table 1). In contrast, throughout a similar time frame, stimulated tear volumes remained fairly constant in male CD-1 mice, a nonautoimmune line used as a control for NOD mice (Figure 1A). Specific data, presented in Figure 1 and Table 1, show two interesting points. First, the weight-compensated tear volumes for CD1 mice did not exhibit any statistically significant differences with age, whereas the weight-compensated tear volumes for both NOD/LtJ and

Table 3. Summary of Differentially Expressed Lacrimal Proteins in NOD/LtJ versus CD-1 Mice at Various Ages

Age at comparison (weeks)	Total number of proteins analyzed	Unique to NOD/LtJ	Increased in NOD/LtJ	Approximately equally expressed	Increased in CD-1	Unique to CD-1
8 to 10	65	2	14	13	19	17
12 to 16	112	5	30	31	37	9
21	81	3	27	15	25	11

Table 4. Major Proteins Identified by Tandem MS/MS from the Gel of Tear Proteins from Older CD1 and NOD Lt/J Mice Shown in Figure 5

Spot no.	Descriptive name	Accession no.	Mr (kd) Theor.	Observ.	PI Theor.	Observ.	Seq. cov. (%)
2	Lacrimal androgen-binding protein δ	IPI00466514	12.2	12	4.4	3.5	22.2
3	Similar to prostatic steroid-binding protein C1 chain precursor	IPI00664264	12.0	12	6.5	5.2	45.4
4	Cystatin Ap5 precursor	IPI00420893	20.6	16	7.7	7.2	31.8
18	Lactoperoxidase	IPI00133770	80.9	69	7.2	5	11.5
19	Lactoperoxidase	IPI00133770	80.8	69	7.2	5.1	2.7
	Keratin, type I cytoskeletal 15	IPI00225378	49.5	69	4.9	5.1	3.5
20	Lactoperoxidase	IPI00133770	80.8	69	7.2	5.2	3.2
21	Similar to triacylglycerol lipase, gastric precursor	IPI00348851	91.2	35	7.0	4.9	5.7
22	Similar to triacylglycerol lipase, gastric precursor	IPI00348851	91.2	35	7.0	4.75	5.7
25	Odorant binding protein 1a	IPI00187557	18.5	16	5.7	5.65	23
26	Seminal vesicle autoantigen	IPI00118165	16.0	12	6.5	5.6	42.4
27	Lacrimal androgen-binding protein ϵ	IPI00411016	12.9	11	5.9	5.65	53.5
29	Lacrimal androgen-binding protein ϵ	IPI00411016	12.9	11	5.9	5.5	24.6
30	Odorant binding protein 1a	IPI00187557	18.5	15	5.7	5.1	42.3
31	Odorant binding protein 1a	IPI00187557	18.5	15	5.7	5	27
32	Odorant binding protein 1a	IPI00187557	18.5	23	5.7	5.35	27
	Lipocalin 11	IPI00275210	19.4	23	5.7	5.35	32.9
33	Lipocalin 11	IPI00275210	19.4	20	5.7	5.35	25
35	Major urinary protein 4	IPI00115241	20.5	20	5.8	5.3	20.2
37	Odorant binding protein 1a	IPI00187557	18.5	18	5.7	5.2	11
38	Major urinary protein 4 precursor	IPI00115241	20.5	20	5.8	5.6	37.6
42	Lipocalin 11	IPI00275210	19.4	21	5.7	5.2	16.3
48	Prolactin-inducible protein homolog precursor	IPI00113711	16.8	13	4.8	4.9	51.4
57	Deoxyribonuclease 1 precursor	IPI00308684	32	25	4.9	4.75	12.3
58	Uncharacterized protein C6ORF58 homolog precursor	IPI00471102	38	32	4.4	4.2	10.7
59	Uncharacterized protein C6ORF58 homolog precursor	IPI00471102	38	32	4.4	4	8.6

Proteins shown here were identified by distinct peptide ion spectra representing two or more peptides representing that particular protein in the SEQUEST algorithm results. Peptides were matched to entries in the IPI mouse v1.31 (October 2004) database. Proteins identified by one distinct peptide ion spectrum are shown in Supplemental Table 1 (see *http://ajp.amjpathol.org*).

*Indicates a modified amino acid, whereas a period indicates that the amino acid residue prior to this one was not identified.

†The fold change of the ratio of the normalized volume of spots from NOD Lt/J and CD1. Negative values mean down-regulation in NOD Lt/J, and positive values indicate up-regulation in the NOD Lt/J.

(table continues)

Table 4. *Continued*

Peptides identified	NOD/CD1†	Function
R.NVYNFYNNGK.Y, K.YLSNIK.S, K.DISSPIIFK.I, K.LASCPFNEQADQHKK.T, K.TNCFIEVYNEVSPNVK.L	NOD only	Secretoglobin, function unknown as yet,[45] in the rodents may serve as a pheromone[46]
K.DLALFLLGSK.E, K.ESLEEDLK.T, K.ESLEEDLKTYNPPQEVIDAK.M, K.TYNPPQEVIDAK.M, K.ECVDNISYADR.I, K.ILGECGVK.A,	−5.2	Peptide C1 forms part of the a-subunit of prostate binding protein. Secretory function in luminal prostate cells[47]
R.NVYNFYNNGK.Y, K.YLSNIK.S, K.DISSPIIFK.I, K.LASCPFNEQADQHKK.T, K.TNCFIEVYNEVSPNVK.L	−9.0	Cysteine protease inhibitor[48]
R.HLSDYLK.H, R.EQINALTSFLDASLVYSPEPSLANR.L, R.ASEQILLATSHTLFIR.E, R.ISNVFTFALR.F, K.DGGIDPLVR.G, K.TLEELSAVM*K.N, K.TLEELSAVM*KNEVLAK.K	−33.6	Bacteriostatic against streptococci and lactobacilli. No antibacterial effect on it s own but has ability to oxidize SCN^- in the presence of H_2O_2[49]
R.AFCGLSQPK.T, R.LVCDNTGIDK.V	−32.8	Bacteriostatic against streptococci and lactobacilli. No antibacterial effect on it s own but has ability to oxidize SCN^- in the presence of H_2O_2[49]
K.VTMQNLNDR.L, R.LASYLDK.V		Intermediate filament protein
R.KNPALGSANR.A, R.DYLPILLGDEM*QK.W	−32.6	*Vide supra*
K.LSILIAPIHTVK.Y, R.LPAYFTPTAFK.S	CD1 only	Digestion of triacylglycerols
R.LPAYFTPTAFK.S, R.EEVSEEILTILR.K	CD1 only	Digestion of triacylglycerols
K.TVAIAADRVDK.I, K.TVAIAADRVDKIER.G, K.VTFYVNENGQCSLTTITGYLQEDGK.T	−3.32	Subclass of lipocalins. Reversibly bind odorants and pheromones[50,51]
K.GKNEFTVTLQVK.N, K.VSTVMNPSIK.Y, K.VSTVM*NPSIK.Y, K.YLSAHAIYTSCLCSANK.Y, K.SICPDDEKIFPVTSYVETATQK.I, K.IFPVTSYVETATQK.I	2.52	Glycoprotein found in murine seminal plasma, suppresses the motility of sperm. In saliva plays a major role in host defense by binding to microorganisms such as Streptococcus[52]
R.IGLHTELAPFDPTVEEK.E, R.IGLHTELAPFDPTVEEKEAFEK.I, K.IQDCYEEEGLKAK.T, K.TEDM*KLM*TTILFSSECR.S, K.LM*TTILFSSECR.S, K.EVLKNILVK.F	−1.2	
R.IGLHTELAPFDPTVEEK.E, K.IQDCYEEEGLK.A	−1.3	
K.TVAIAADR.V, K.TVAIAADRVDK.I, K.VTFYVNENGQCSLTTITGYLQEDGK.T, K.LVDESPENLTFYSENVDR.A, K.LLFILGHGPLTSEQK.E	−3.3	*Vida supra*
K.TVAIAADRVDKIER.G, R.YKLVDESPENLTFYSENVDR.A, K.EKFAELAEEK.G	−2.8	*Vida supra*
K.TVAIAADRVDKIER.G, R.YKLVDESPENLTFYSENVDR.A, K.EKFAELAEEK.G	NOD only	*Vida supra*
R.SLIEEGGAYR.C, K.EFYIAEK.T, K.TDTPGQYTFEYQGR.N, R.SLSTDELGWER.Y, R.GIAPENIVDLSLSR.R		Anti-microbial binds to microbial siderophores[53]
R.SLIEEGGAYR.C, K.CVKEFYIAEK.T, K.EFYIAEK.T, R.SLSTDELGWER.Y, R.GIAPENIVDLSLSR.R	3.2	Anti-microbial binds to microbial siderophores[53]
K.TFQLM*ELYGR.K, R.KADLNSDIK.E, K.LCEEHGIIK.E, K.ENIIDLTK.T	1.5	Carrier for volatile nonpolar pheromones[54] Synthesis in larcimal gland is regulated by testosterone[55]
K.FAELAEEK.G, R.EVLITDYCPE.-	1.4	*Vide supra*
R.VFVEHIHVLENSLAFK.F, K.FHTVIDGECSEIFLVADK.T, K.AGEYSVM*YDGFNTFTILK.T, K.TDYDNYIM*FHLINEK.D	2.5	*Vide supra*
K.TDTPGQYTFEYQGR.N, R.RGIAPENIVDLSLSR.R, R.GIAPENIVDLSLSR.R	NOD only	*Vida supra*
K.AYLVSNEPM*EGAFNYVQTR.C, R.CLCNDHPIR.F, R.FFWDIIITR.T, R.TVTFATVIDIVR.E, R.EKNICPNDM*AVVPITANR.Y, K.NICPNDM*AVVPITANR.Y, R.YYTYNTVR.M	11.3	Aspartyl proteinase. Acinar protein, synthesis in male lacrimal gland regulated by testosterone.[56] Binds oral and nonoral bacteria. PIP is an aspartyl proteinase and it acts as a factor capable of suppressing T-cell apoptosis through its interaction with CD4.[52]
R.IAAFNIR.T, R.YDIAVIQEVR.D, R.DSHLVAVGK.L, R.YVVSEPLGR.K	4.7	Catalyzes the hydrolytic cleavage of phosphodiester linkages in the DNA backbone
R.ILLEETAM*YFAK.Y, R.YNFYSEK.E, R.NSGSLSLTLWENLM*STK.L	NOD only	Unknown
R.ILLEETAM*YFAK.Y, R.YNFYSEK.E, K.AFEEFLATSS.-	NOD only	Unknown

NOD.B10-*H2*^{b} mice showed statistically significant decreases with age ($P < 0.01$ and $P < 0.05$, respectively). Second, despite progression of disease in the NOD/LtJ and NOD.B10-*H2*^{b} mice, both strains retained measurable lacrimal gland function throughout the observed time frame. Both the NOD/LtJ and the NOD.B10 mice showed an early statistically significant (using Student's *t*-test) decrease in tear volumes: 4-week-old (1.60 ± 0.10 μl/g) versus 8-week-old (1.10 ± 0.13 μl/g) NOD/LtJ mice ($P < 0.05$) and 5-week-old (1.54 ± 0.38 μl/g) versus 13-week-old (1.02 ± 0.09 μl/g) NOD.B10-*H2*^{b} mice ($P < 0.05$).

Histopathological Analysis of the Ocular-Associated Exocrine Gland System

Leukocyte infiltration of the submandibular gland is a critical criterion for identification of the autoimmune phase of SjS in both human and animal models. Although the absolute number of lymphocytic foci present in the salivary and/or lacrimal glands often does not correlate directly with disease or its severity, NOD-derived mouse strains exhibiting SjS-like disease typically have leukocytic infiltrates in their lacrimal glands.[22] To define temporal changes in leukocyte infiltration within the ocular-associated exocrine glands of NOD/LtJ and NOD.B10-*H2*^{b} mice, the extra- and intraorbital lacrimal glands, the meibomian glands, and the Hardarian glands were freshly excised from male mice euthanized at various ages between 4 and 36 weeks, fixed in formalin, embedded in paraffin, sectioned, and stained with H&E. Histological examinations of the extraorbital lacrimal glands revealed that multiple foci of leukocytic infiltrates were easily detected as early as 7 weeks of age in NOD/LtJ and NOD.B10-*H2*^{b} mice. The infiltrates continued to increase in number and size with time (Figure 2 and Table 2). However, the infiltrates eventually began to coalesce as the disease became more severe leading to a decrease in the overall number, which is noticeable in the NOD/LtJ. Thus, the decline in tear production seems to occur concomitantly with the appearance of infiltrates within the lacrimal glands of NOD/LtJ and NOD.B10-*H2*^{b} mice. Nevertheless, large numbers of exocrine cells persisted within these glands until the end of the study at ~1 year. As expected, no leukocytic infiltrations were observed in the extraorbital lacrimal glands of CD1 mice up to 40 weeks of age. A quantitative comparison of the number and grading of lymphocytic foci in NOD/LtJ and NOD.B10-*H2*^{b} mice throughout time is presented in Table 2.

Immunohistochemical staining revealed that the leukocytic foci present in the lacrimal glands of NOD/LtJ and NOD.B10-*H2*^{b} mice were comprised of distinct regions of $CD3^+$ T cells and $B220^+$ B cells localized in well-defined foci (Figure 3). Interestingly, the leukocytic foci observed in the lacrimal glands of young NOD/LtJ and NOD.B10-*H2*^{b} mice are comprised mostly of T cells surrounded by B cells. Throughout time T cells became less numerous and more scattered in the multilobular lesions whereas B-cell frequencies remained strong.

H&E staining of the Hardarian, meibomian, and intraorbital lacrimal glands of NOD/LtJ and NOD.B10-*H2*^{b} mice also revealed differences when compared with the glands of CD-1 mice (Figure 4). Again, leukocytic infiltrates were clearly present within the intraorbital lacrimal glands of NOD/LtJ and NOD.B10-*H2*^{b} mice, whereas only an occasional infiltrate could be found within the intraorbital lacrimal glands of CD1 mice. No infiltrates were present in the Hardarian glands. In contrast, small leukocyte aggregates were observed occasionally in meibomian glands of NOD/LtJ and NOD.B10-*H2*^{b} mice (Figure 4).

Profiling Temporal Changes in Tear Proteins Using 2-D DIGE and Tandem Mass Spectrometry

To determine whether any temporal changes in the general protein composition of tears occur with development of SjS-like disease, tear protein profiles were studied with tear fluids collected from either CD1 or NOD/LtJ mice of various ages after stimulations with pilocarpine. For this analysis, individual tear samples collected from mice within each experimental group were pooled to minimize individual mouse variability. An example of a protein profile for tears from 21-week-old CD1 and NOD/LtJ mice after separation by 2D DIGE is presented in Figure 5A showing the false-color image of the differently labeled samples. Figure 5, C and D, shows the overlay that reveals differential quantities of individual protein spots. This analysis was also performed on tears from 8- to 10-week-old and 12- to 16-week-old mice representing onset and development of SjS stages in the NOD mouse model. The temporal changes observed in the number of spots between NOD/LtJ and CD1 mice with respect to both age and onset of SjS-like disease in NOD/LtJ mice are summarized in Table 3. Distinct differences in spot distribution at each time point examined during development of SjS-like disease proved unique, suggesting (but not proving) that the progression of the disease involves different physiological entities that could translate to specific markers of disease development. To determine proteins that were being differentially expressed in the disease state, equal quantities of tear proteins from the 21-week-old CD1 and NOD/LtJ mice were labeled with Cy3 and Cy5, respectively. The two labeled samples were mixed, and additional amounts of unlabeled CD1 and NOD/LtJ tear protein were added to ensure sufficient material for biomarker identification of individual spots by Coomassie Blue staining and mass spectroscopy identification (Figure 5B). Of a total of 180 spots, 63 spots from the gel representing the mice of the older mice were picked for identification by tandem mass spectrometry. Of these, 23 were positively identified by the presence of two or more peptides representing that particular protein (listed in Table 4). The peptide ion mass spectra used to obtain the data in Table 4 had Xcorr values in the range of 1.8 to 5.2 with a ΔCn span in the range of 0.08 to 0.64. There were several proteins identified on the basis of one peptide spectrum, and these are shown in Supplemental Table 1 (see *http://ajp.amjpathol.org*). Prominent among

those proteins identified are the secretoglobins, proteases, and many lipid-binding anti-bacterial proteins. Specifically, we observed increases in lipocalin 11, prolactin-inducible protein, seminal vesicle autoantigen, odorant-binding protein 1a, and decreases in cystatin Ap5 and lactoperoxidase in the disease relative to control state. There was an apparent modification in the expression and/or posttranslational modifications of lacrimal androgen-binding proteins in the NOD/LtJ tears and a complete lack of the acinar protein triglycerol lipase gastric precursor, which was only found in the tear proteome of the CD1 strain. There was also an increase in deoxyribonuclease in the NOD/LtJ strain, mostly likely attributable to acinar cell destruction and apoptosis.[35] As is common in 2D DIGE analysis, some spots did not purely represent a single protein, and there were several instances of co-migration. In particular, both odorant-binding protein 1a and lipocalin were identified in spot 32. Many of the minor proteins of lower molecular weight were seen to cluster around spot 30 (Supplemental Table 1; see *http://ajp.amjpathol.org*). The problem of co-migration confounds the ability to specifically define differences in expression of these proteins between control and disease state; however, they offer interesting possibilities to explore as potential biomarkers.

Discussion

In the present study, we have attempted to correlate three parameters that when taken together should provide a comprehensive picture of autoimmune xerophthalmia in the NOD mouse model of SjS in humans. These three parameters are i) the temporal and progressive loss of stimulated tear flow rates observed in both NOD/LtJ and NOD.B10-*H2*^{b} mice; ii) the appearance and expansion of leukocytic infiltrations of the lacrimal glands (as well as other ocular-associated secretory organs); and iii) the temporal changes in the protein composition of tears. Using the nonautoimmune strain CD1 as a control, we have been able to make both inter- and intragroup comparisons. Results clearly suggest a direct correlation between these three parameters and that the development and onset of disease is a progressive phenomenon measurable by distinct physiological changes. With this in mind then, there exists multiple opportunities to develop profiles of SjS at various stages of development, one of the long-range goals of this field.

Diagnosis of SjS according to the recently revised criteria[36] includes histopathological analysis of infiltrating lymphocytes in a labial gland lip biopsy sample.[2,4] Lacrimal gland biopsies are approved according to the Japanese criteria for diagnosis of Sjögren's syndrome.[37] Infiltrates appear as periductal foci within the glandular architecture of the lacrimal and salivary glands.[38] Although it has long been accepted that the lymphocytes infiltrating the lacrimal and salivary tissues are predominantly CD4$^+$ T cells with a smaller B and CD8$^+$ T-cell component, more recent data suggest a major infiltration of B cells during the early development of the disease, a fact reinforced in the present studies. Histologically, the lymphocytic infiltrations (or foci) that appear in the lacrimal glands show by immunofluorescent staining that, throughout time, the lesion evolves from a B-cell-centered focus surrounded by T cells at 12 to 16 weeks of age to a predominantly B-cell focus at 33 weeks of age.

Most often, though, keratoconjunctivitis sicca (dry eyes) is assessed by specific tests for changes in lacrimal flow rates and biochemical changes in protein composition. Analyses of these two items in the present study revealed that, as tear production decreased in the NOD/LtJ and NOD.B10-*H2*^{b} mice, major changes occurred in the tear protein composition reflecting lacrimal gland dysfunction. Our results showing the increase in major protein components are in agreement with previously published data showing increases in lipocalin and lysozyme in dry eye patients.[39] Likewise, we observed increases in the amounts of lipid-binding anti-bacterial proteins in NOD/LtJ lacrimal secretions. Lipocalin 11, seminal vesicle autoantigen, and prolactin-inducible protein have been shown to bind to and inactivate bacteria. Similarly, there are decreases in cellular products of the acinar tissue, in particular prostatic steroid-binding protein, lactoperoxidase, the odorant-binding proteins, triacylglycerol lipase, and cystatin Ap5. An increase in the amount of deoxyribonuclease in the disease state could be associated with the acinar cell destruction observed in the histological analysis.

Markusse and colleagues[40] have shown that tear fluid levels of lactoferrin and α-1-antitypsin were increased whereas those of peroxidase, lysozyme, and amylase were decreased in primary SjS patients relative to non-SjS patients. Similarly, Ohashi et al[41] found higher levels of lactoferrin with lower levels of epidermal growth factor and aquaporin 5 correlated with severity of dry eye disease in SjS patients as measured by either the Schirmer or Rose Bengal tests. Tomosugi and colleagues[42] identified 10 specific proteins that exhibited altered expression levels in primary SjS patients relative to healthy age- and gender-matched volunteers. Of these 10 proteins, lysozyme and albumin were down-regulated. Despite the consistent observation that lactoferrin is increased in tear fluids of SjS patients, it is not likely to be used as a specific disease marker because significant increases in saliva levels are also seen in patients with type-2 diabetes[43] and non-SjS dry-eye disease. In studying disease progression, a more promising approach might be the examination of overall profiles in which predictable patterns or changes in patterns are associated with various disease stages.[44] In the present study, 2D-DIGE analyses combined with mass spectrometry determination of proteins present in lacrimal secretions from NOD/LtJ mice in advanced stage of the disease clearly show a distinct protein profile when compared with CD1 controls. This observation is consistent with human SjS disease and substantiates the advantages in examining lacrimal as well as salivary secretions for potential SjS biomarkers in the human condition.

Last, the significant decreases in tear secretions observed in the NOD/LtJ mice between 4 and 8 weeks of age coincide with the appearance of infiltrates observed in the lacrimal glands as early as 6 to 7 weeks of age. In conclusion, direct correlations exist between i) loss of secretory

function, ii) increased severity of leukocytic infiltrations, and iii) the temporal changes in tear protein profiles observed for the NOD/LtJ. Because significant changes in the quantities and posttranslational modifications occur in major tear proteins, a substantial number of lower molecular weight proteins needs to be explored further as potential markers of disease progression. Thus, it is apparent that more direct quantitative mass spectrometry is required to eliminate the complication of co-migration and thus to allow clear definition of differences in protein expression between SjS patients and control patients. The possibility of identifying candidate markers in lacrimal secretions, for early diagnosis of SjS, would prove useful in establishing risk factors and diagnostic tools for following development and onset of disease within at-risk populations.

Acknowledgments

We thank Dr. Li-jun Yang for sharing her expertise in histopathology; Ms. Janet Cornelius and Ms. Pat Glenton for their contributions in breeding and maintaining the mice used in this study, as well as for valuable technical assistance; Marjorie Chow for performing the 2D DIGE; and Drs. Stanley Stevens, Sophie Alvarez, and Scott McClung, the University of Florida's Proteomics Core Facility, for performing the tandem mass spectrometry.

References

1. Lemp MA: Report of the National Eye Institute/Industry Workshop on Clinical Trials in Dry Eyes. Clao J 1995, 21:221–232
2. Dogru M, Stern ME, Smith JA, Foulks GN, Lemp MA, Tsubota K: Changing trends in the definition and diagnosis of dry eyes. Am J Ophthalmol 2005, 140:507–508
3. Dogru MT, Tsubota K: New insights into the diagnosis and treatment of dry eye. Ocular Surface 2004, 2:59–75
4. Fox RI: Sjogren's syndrome. Lancet 2005, 366:321–331
5. Fox PC, Speight PM: Current concepts of autoimmune exocrinopathy: immunologic mechanisms in the salivary pathology of Sjogren's syndrome. Crit Rev Oral Biol Med 1996, 7:144–158
6. Fox RI, Kang HI: Pathogenesis of Sjogren's syndrome. Rheum Dis Clin North Am 1992, 18:517–538
7. Whitacre CC: Sex differences in autoimmune disease. Nat Immunol 2001, 2:777–780
8. Toda I, Wickham LA, Sullivan DA: Gender and androgen treatment influence the expression of proto-oncogenes and apoptotic factors in lacrimal and salivary tissues of MRL/lpr mice. Clin Immunol Immunopathol 1998, 86:59–71
9. Warren DW, Azzarolo AM, Huang ZM, Platler BW, Kaswan RL, Gentschein E, Stanczyk FL, Becker L, Mircheff AK: Androgen support of lacrimal gland function in the female rabbit. Adv Exp Med Biol 1998, 438:89–93
10. Wickham LA, Rocha EM, Gao J, Krenzer KL, da Silveira LA, Toda I, Sullivan DA: Identification and hormonal control of sex steroid receptors in the eye. Adv Exp Med Biol 1998, 438:95–100
11. Sullivan DA: Tearful relationships? Sex, hormones, the lacrimal gland, and aqueous-deficient dry eye. Ocul Surf 2004, 2:92–123
12. Nguyen CQ, Cha SR, Peck AB: Sjogren's syndrome (SjS)-like disease of mice: the importance of B lymphocytes and autoantibodies. Front Biosci 2007, 12:1767–1789
13. Cha S, Singson E, Cornelius J, Yagna JP, Knot HJ, Peck AB: Muscarinic acetylcholine type-3 receptor desensitization due to chronic exposure to Sjogren's syndrome-associated autoantibodies. J Rheumatol 2006, 33:296–306
14. Brayer JB, Cha S, Nagashima H, Yasunari U, Lindberg A, Diggs S, Martinez J, Goa J, Humphreys-Beher MG, Peck AB: IL-4-dependent effector phase in autoimmune exocrinopathy as defined by the NOD.IL-4-gene knockout mouse model of Sjogren's syndrome. Scand J Immunol 2001, 54:133–140
15. Cha S, Brayer J, Gao J, Brown V, Killedar S, Yasunari U, Peck AB: A dual role for interferon-gamma in the pathogenesis of Sjogren's syndrome-like autoimmune exocrinopathy in the nonobese diabetic mouse. Scand J Immunol 2004, 60:552–565
16. Gao J, Killedar S, Cornelius JG, Nguyen C, Cha S, Peck AB: Sjogren's syndrome in the NOD mouse model is an interleukin-4 time-dependent, antibody isotype-specific autoimmune disease. J Autoimmun 2006, 26:90–103
17. Robinson CP, Yamamoto H, Peck AB, Humphreys-Beher MG: Genetically programmed development of salivary gland abnormalities in the NOD (nonobese diabetic)-scid mouse in the absence of detectable lymphocytic infiltration: a potential trigger for sialoadenitis of NOD mice. Clin Immunol Immunopathol 1996, 79:50–59
18. Brayer JB, Humphreys-Beher MG, Peck AB: Sjogren's syndrome: immunological response underlying the disease. Arch Immunol Ther Exp (Warsz) 2001, 49:353–360
19. Cha S, Peck AB, Humphreys-Beher MG: Progress in understanding autoimmune exocrinopathy using the non-obese diabetic mouse: an update. Crit Rev Oral Biol Med 2002, 13:5–16
20. Cha S, van Blockland SC, Versnel MA, Homo-Delarche F, Nagashima H, Brayer J, Peck AB, Humphreys-Beher MG: Abnormal organogenesis in salivary gland development may initiate adult onset of autoimmune exocrinopathy. Exp Clin Immunogenet 2001, 18:143–160
21. Robinson CP, Cornelius J, Bounous DE, Yamamoto H, Humphreys-Beher MG, Peck AB: Characterization of the changing lymphocyte populations and cytokine expression in the exocrine tissues of autoimmune NOD mice. Autoimmunity 1998, 27:29–44
22. Robinson CP, Cornelius J, Bounous DI, Yamamoto H, Humphreys-Beher MG, Peck AB: Infiltrating lymphocyte populations and cytokine production in the salivary and lacrimal glands of autoimmune NOD mice. Adv Exp Med Biol 1998, 438:493–497
23. Nguyen KH, Brayer J, Cha S, Diggs S, Yasunari U, Hilal G, Peck AB, Humphreys-Beher MG: Evidence for antimuscarinic acetylcholine receptor antibody-mediated secretory dysfunction in nod mice. Arthritis Rheum 2000, 43:2297–2306
24. Robinson CP, Brayer J, Yamachika S, Esch TR, Peck AB, Stewart CA, Peen E, Jonsson R, Humphreys-Beher MG: Transfer of human serum IgG to nonobese diabetic Igmu null mice reveals a role for autoantibodies in the loss of secretory function of exocrine tissues in Sjogren's syndrome. Proc Natl Acad Sci USA 1998, 95:7538–7543
25. Gilbard JP, Hanninen LA, Rothman RC, Kenyon KR: Lacrimal gland, cornea, and tear film in the NZB/NZW F1 hybrid mouse. Curr Eye Res 1987, 6:1237–1248
26. Jabs DA, Prendergast RA: Murine models of Sjogren's syndrome. Immunohistologic analysis of different strains. Invest Ophthalmol Vis Sci 1988, 29:1437–1443
27. Haneji N, Nakamura T, Takio K, Yanagi K, Higashiyama H, Saito I, Noji S, Sugino H, Hayashi Y: Identification of alpha-fodrin as a candidate autoantigen in primary Sjogren's syndrome. Science 1997, 276:604–607
28. Takada K, Takiguchi M, Inaba M: Different effects on the inflammatory lesions in the lacrimal and salivary glands after neonatal thymectomy in IQI/Jic mice, a model for Sjogren's syndrome. J Vet Med Sci 2005, 67:955–957
29. Takada K, Takiguchi M, Konno A, Inaba M: Spontaneous development of multiple glandular and extraglandular lesions in aged IQI/Jic mice: a model for primary Sjogren's syndrome. Rheumatology (Oxford) 2004, 43:858–862
30. Li H, Dai M, Zhuang Y: A T cell intrinsic role of Id3 in a mouse model for primary Sjogren's syndrome. Immunity 2004, 21:551–560
31. Shim GJ, Warner M, Kim HJ, Andersson S, Liu L, Ekman J, Imamov O, Jones ME, Simpson ER, Gustafsson JA: Aromatase-deficient mice spontaneously develop a lymphoproliferative autoimmune disease resembling Sjogren's syndrome. Proc Natl Acad Sci USA 2004, 101:12628–12633
32. Batten M, Fletcher C, Ng LG, Groom J, Wheway J, Laabi Y, Xin X, Schneider P, Tschopp J, Mackay CR, Mackay F: TNF deficiency fails to protect BAFF transgenic mice against autoimmunity and reveals a predisposition to B cell lymphoma. J Immunol 2004, 172:812–822
33. Wicker LS, Appel MC, Dotta F, Pressey A, Miller BJ, DeLarato NH, Fischer PA, Boltz Jr RC, Peterson LB: Autoimmune syndromes in major histocompatibility complex (MHC) congenic strains of nono-

bese diabetic (NOD) mice. The NOD MHC is dominant for insulitis and cyclophosphamide-induced diabetes. J Exp Med 1992, 176:67–77
34. Hamano T, Mitsunaga S, Kotani S, Hamano T, Hamano K, Hamano H, Sakamoto R, Tamura H: Tear volume in relation to contact lens wear and age. Clao J 1990, 16:57–61
35. Gaipl US, Sheriff A, Franz S, Munoz LE, Voll RE, Kalden JR, Herrmann M: Inefficient clearance of dying cells and autoreactivity. Curr Top Microbiol Immunol 2006, 305:161–176
36. Vitali C, Bombardieri S, Jonsson R, Moutsopoulos HM, Alexander EL, Carsons SE, Daniels TE, Fox PC, Fox RI, Kassan SS, Pillemer SR, Talal N, Weisman MH: Classification criteria for Sjogren's syndrome: a revised version of the European criteria proposed by the American-European Consensus Group. Ann Rheum Dis 2002, 61:554–558
37. Kawai Y, Sumi M, Kitamori H, Takagi Y, Nakamura T: Diffusion-weighted MR microimaging of the lacrimal glands in patients with Sjogren's syndrome. Am J Roentgenol 2005, 184:1320–1325
38. Parkin B, Chew JB, White VA, Garcia-Briones G, Chhanabhai M, Rootman J: Lymphocytic infiltration and enlargement of the lacrimal glands: a new subtype of primary Sjogren's syndrome? Ophthalmology 2005, 112:2040–2047
39. Grus FH, Podust VN, Bruns K, Lackner K, Fu S, Dalmasso EA, Wirthlin A, Pfeiffer N: SELDI-TOF-MS ProteinChip array profiling of tears from patients with dry eye. Invest Ophthalmol Vis Sci 2005, 46:863–876
40. Markusse HM, van Haeringen NJ, Swaak AJ, Hogeweg M, de Jong PT: Tear fluid analysis in primary Sjogren's syndrome. Clin Exp Rheumatol 1993, 11:175–178
41. Ohashi Y, Ishida R, Kojima T, Goto E, Matsumoto Y, Watanabe K, Ishida N, Nakata K, Takeuchi T, Tsubota K: Abnormal protein profiles in tears with dry eye syndrome. Am J Ophthalmol 2003, 136:291–299
42. Tomosugi N, Kitagawa K, Takahashi N, Sugai S, Ishikawa I: Diagnostic potential of tear proteomic patterns in Sjogren's syndrome. J Proteome Res 2005, 4:820–825
43. Dodds MW, Yeh CK, Johnson DA: Salivary alterations in type 2 (non-insulin-dependent) diabetes mellitus and hypertension. Community Dent Oral Epidemiol 2000, 28:373–381
44. Ryu OH, Atkinson JC, Hoehn GT, Illei GG, Hart TC: Identification of parotid salivary biomarkers in Sjogren's syndrome by surface-enhanced laser desorption/ionization time-of-flight mass spectrometry and two-dimensional difference gel electrophoresis. Rheumatology (Oxford) 2006, 45:1077–1086
45. Remington SG, Nelson JD: Secretoglobins: sexually dimorphic expression of androgen-binding protein mRNA in mouse lacrimal glands. Invest Ophthalmol Vis Sci 2005, 46:31–38
46. Emes RD, Riley MC, Laukaitis CM, Goodstadt L, Karn RC, Ponting CP: Comparative evolutionary genomics of androgen-binding protein genes. Genome Res 2004, 14:1516–1529
47. Janulis L, Nemeth JA, Yang T, Lang S, Lee C: Prostatic luminal cell differentiation and prostatic steroid-binding protein (PBP) gene expression are differentially affected by neonatal castration. Prostate 2000, 43:195–204
48. Puente XS, Lopez-Otin C: A genomic analysis of rat proteases and protease inhibitors. Genome Res 2004, 14:609–622
49. Conner GE, Salathe M, Forteza R: Lactoperoxidase and hydrogen peroxide metabolism in the airway. Am J Respir Crit Care Med 2002, 166:S57–S61
50. Pes D, Mameli M, Andreini I, Krieger J, Weber M, Breer H, Pelosi P: Cloning and expression of odorant-binding proteins Ia and Ib from mouse nasal tissue. Gene 1998, 212:49–55
51. Tegoni M, Pelosi P, Vincent F, Spinelli S, Campanacci V, Grolli S, Ramoni R, Cambillau C: Mammalian odorant binding proteins. Biochim Biophys Acta 2000, 1482:229–240
52. Yoshida M, Kaneko M, Kurachi H, Osawa M: Identification of two rodent genes encoding homologues to seminal vesicle autoantigen: a gene family including the gene for prolactin-inducible protein. Biochem Biophys Res Commun 2001, 281:94–100
53. Fluckinger M, Haas H, Merschak P, Glasgow BJ, Redl B: Human tear lipocalin exhibits antimicrobial activity by scavenging microbial siderophores. Antimicrob Agents Chemother 2004, 48:3367–3372
54. Bacchini A, Gaetani E, Cavaggioni A: Pheromone binding proteins of the mouse, Mus musculus. Experientia 1992, 48:419–421
55. Shaw PH, Held WA, Hastie ND: The gene family for major urinary proteins: expression in several secretory tissues of the mouse. Cell 1983, 32:755–761
56. Myal Y, Iwasiow B, Yarmill A, Harrison E, Paterson JA, Shiu RP: Tissue-specific androgen-inhibited gene expression of a submaxillary gland protein, a rodent homolog of the human prolactin-inducible protein/GCDFP-15 gene. Endocrinology 1994, 135:1605–1610